DMD Fast Forward. Published on February 2, 2020 as DOI: 10.1124/dmd.119.089003
This article has not been copyedited and formatted. The final version may differ from this version.

Drug interactions for low dose inhaled nemiralisib – a case study integrating modelling, in vitro and clinical investigations

Aarti Patel, Robert Wilson, Andrew W Harrell, Kunal S Taskar, Maxine Taylor, Helen Tracey, Kylie Riddell, Alex Georgiou, Anthony P Cahn, Miriam Marotti, Edith M Hessel

Drug Metabolism and Pharmacokinetics, GlaxoSmithKline R&D, United Kingdom (AP, AWH, KST, MT and HT)
RD Projects Clinical Platforms & Sciences, GlaxoSmithKline R&D, Stevenage, United Kingdom (RW)
Global Clinical and Data Operations, GlaxoSmithKline R&D, Ermington, Australia (KR)
Bioanalysis, Immunogenicity and Biomarkers, GlaxoSmithKline R&D, Ware, United Kingdom (AG)
GlaxoSmithKline, Discovery Medicine, Stevenage, United Kingdom (AC)
Safety and Medical Governance, GlaxoSmithKline R&D, Stockley Park, Uxbridge, United Kingdom (MM)
Refractory Respiratory Inflammation Discovery Performance Unit, GlaxoSmithKline, Stevenage, United Kingdom (EMH)

Running title: Drug interactions for inhaled nemiralisib

Corresponding author: Aarti Patel. Drug Metabolism and Pharmacokinetics, GlaxoSmithKline R&D, United Kingdom. Email: aarti.2.patel@gsk.com

DMD Fast Forward. Published on February 2, 2020 as DOI: 10.1124/dmd.119.089003
This article has not been copyedited and formatted. The final version may differ from this version.

Number of pages: 46

Number of tables: 5

Number of figures: 3

Number of references: 19

Abstract word count: 250

Introduction word count: 749

Discussion word count: 1347

Abbreviations

ADME: absorption, distribution, metabolism and excretion; AE: adverse event; AUC: area under the plasma concentration time curve; $AUC_{0\text{-}inf}$: area under the plasma concentration time curve from time zero extrapolated to infinite time; BMI: body mass index; BCRP: breast cancer resistance protein; CI: confidence interval; C_{max}: maximum observed plasma concentration; CYP: cytochrome P450; DDI: drug-drug interaction; ECG: electrocardiogram; E2G: estradiol 17β-D-glucuronide; ES: estrone sulfate; FDA: Food and Drug Administration; GlaxoSmithKline: GSK; HEK293: human embryonic kidney mammalian; HLQ: higher limit of quantification; HLM: human liver microsome; HLuM: human lung microsome; IC_{50}: half maximal inhibitory concentration; $I_{max,u}$: maximum unbound systemic concentration; K_i: inactivator concentration to achieve half-maximal inactivation rate; k_{inact}: maximal rate constant of inactivation; K_m: concentration of substrate that leads to half-maximal velocity; LLC-PK1: porcine kidney epithelial cell line; LLQ: lower limit of quantification; MDI: metabolism dependent inhibition; MATE: multidrug and toxin extrusion; MPPD: multiple path particle disposition; NADP+: β-nicotinamide adenine dinucleotide

DMD Fast Forward. Published on February 2, 2020 as DOI: 10.1124/dmd.119.089003
This article has not been copyedited and formatted. The final version may differ from this version.

phosphate; NADPH: nicotinamide adenine dinucleotide phosphate hydrate; OAT: organic anion transporter; OATP: organic anion transporting polypeptide; OCT: organic cation transporter; PAH: p-Aminohippuric acid; P-gp: P-glycoprotein; PI3Kδ: phosphoinositide 3-kinase delta; PBPK: physiologically based pharmacokinetic; PK: pharmacokinetic; rCYP: recombinant CYP enzymes; ROI: region of interest; t_{max}: time to maximum observed plasma concentration; UPLC-LC/MS: ultra performance liquid chromatography liquid chromatography - mass spectrometry; UHPLC-MS/MS: ultra high performance liquid chromatography tandem mass spectrometry

DMD Fast Forward. Published on February 2, 2020 as DOI: 10.1124/dmd.119.089003
This article has not been copyedited and formatted. The final version may differ from this version.

Abstract

In vitro data for low dose inhaled phosphoinositide 3-kinase delta inhibitor nemiralisib revealed that it as a substrate and a potent metabolism-dependent inhibitor of cytochrome P450 (CYP)3A4 and a P-gp substrate. An integrated in silico, in vitro and clinical approach including a clinical drug interaction study, along with a bespoke physiologically based pharmacokinetic (PBPK) model was used to assess the drug-drug interaction (DDI) risk. Inhaled nemiralisib (100 µg, single dose) was co-administered with itraconazole, a potent CYP3A4/P-gp inhibitor, following 200 mg daily administrations for 10 days in 20 male healthy subjects. Systemic exposure to nemiralisib ($AUC_{0\text{-}inf}$) increased by 2.01-fold versus nemiralisib alone. In order to extrapolate the clinical data to other CYP3A4 inhibitors, an inhaled PBPK model was developed using SimCYP® software. Retrospective simulation of the victim risk showed good agreement between simulated and observed data ($AUC_{0\text{-}inf}$ ratio 2.3 versus 2.01, respectively). Prospective DDI simulations predicted a weak but manageable drug interaction when nemiralisib was co-administered with other CYP3A4 inhibitors such as the macrolides clarithromycin and erythromycin (simulated $AUC_{0\text{-}inf}$ ratio of 1.7), both common co-medications in the intended patient populations. PBPK and static mechanistic models were also used to predict a negligible perpetrator DDI effect for nemiralisib on other CYP3A4 substrates including midazolam (a sensitive probe substrate of CYP3A4) and theophylline (a narrow therapeutic index drug and another common co-medication). In summary, an integrated in silico, in vitro and clinical approach including an inhalation PBPK model has successfully discharged any potential patient DDI risks in future nemiralisib clinical trials.

DMD Fast Forward. Published on February 2, 2020 as DOI: 10.1124/dmd.119.089003
This article has not been copyedited and formatted. The final version may differ from this version.

DMD Fast Forward. Published on February 2, 2020 as DOI: 10.1124/dmd.119.089003
This article has not been copyedited and formatted. The final version may differ from this version.

Significance statement

This paper describes the integration of in silico, in vitro and clinical data to successfully discharge potential drug-drug interaction risks for a low dose inhaled drug. This work featured assessment of victim and perpetrator risks of drug transporters and cytochrome P450 (CYP) enzymes utilizing empirical and mechanistic approaches, combined with clinical data (drug interaction and human absorption, metabolism and pharmacokinetics), and physiologically based pharmacokinetic (PBPK) modelling approaches to facilitate bespoke risk assessment in target patient populations.

DMD Fast Forward. Published on February 2, 2020 as DOI: 10.1124/dmd.119.089003
This article has not been copyedited and formatted. The final version may differ from this version.

Introduction

Nemiralisib is a potent and highly selective inhaled phosphoinositide 3-kinase delta (PI3Kδ) inhibitor being investigated as an anti-inflammatory agent in respiratory diseases. In clinical studies, nemiralisib was generally well tolerated across a range of inhalation doses administered to both healthy volunteers and patients (Down et al., 2015; Cahn et al., 2017; Begg et al., 2019; Wilson et al., 2018). Conducting drug-drug interaction (DDI) studies is a required part of a drug's clinical development to assess the potential risk that a drug may either cause a drug interaction as a perpetrator or be affected by another drug as a victim. For any drug interaction investigation, it is therefore important to consider both victim and perpetrator risks. Bloomer et al (2013) emphasize the importance of tailoring any drug interaction investigation to the common co-medications in the intended patient populations and refer to diltiazem (potent P-glycoprotein (P-gp) inhibitor) and verapamil (moderate cytochrome P450 (CYP)3A4 inhibitor and potent P-gp inhibitor) as frequently prescribed co-medications in asthma and chronic obstructive pulmonary disease (COPD). Nemiralisib, however, is a drug under consideration for use in multiple respiratory indications including bronchiectasis and in patients experiencing frequent exacerbations where common co-medications additionally include theophylline (a sensitive narrow therapeutic index CYP3A4 substrate) and the macrolide antibiotics erythromycin and clarithromycin (which are CYP3A4 inhibitors). It was important, therefore, to investigate both victim and perpetrator interactions (particularly for CYP3A4), assessments of which are guided by Food and Drug Administration (FDA, 2017a and 2017b) and European Medicines Agency (EMA, 2012). Clinically relevant victim drug interactions can occur even for low dose inhaled molecules (Foisy et al., 2008) and thus clinical victim interaction studies are an expected feature of an

DMD Fast Forward. Published on February 2, 2020 as DOI: 10.1124/dmd.119.089003
This article has not been copyedited and formatted. The final version may differ from this version.

inhalation clinical development plan. Following the completion of in vitro enzymology and transporter substrate packages (described herein), it was clear that the potential for CYP3A4 and P-gp inhibitors to increase nemiralisib exposure required further investigation, particularly considering the co-medication profile. The most effective way to study a victim drug interaction is through a clinical DDI study. In its clinical drug interaction guidance, FDA (2017a), recommend that a strong index inhibitor should be used to establish a worst-case interaction. Itraconazole is described as both a strong P450 inhibitor and potent P-gp inhibitor which was selected, therefore, as a suitable inhibitor for the study described herein.

FDA (2017b) outlines a tiered approach to investigate perpetrator DDIs which starts with a simple application of basic equations, as described in Supplementary Table S1. If basic thresholds are triggered, then the investigation progresses to more complex static mechanistic models, which are detailed in Supplementary Table S2. The use of qualified PBPK models are an option provided in FDA (2017b) should the static mechanistic models also reveal a DDI risk. Should all these approaches indicate a DDI risk then a clinical perpetrator DDI study may be necessary. Concern thresholds are rarely, if ever, triggered for low dose inhaled molecules where systemic exposure is extremely low. Despite this, it remains an expectation from some regulators that in vitro data is presented for inhaled molecules and for drug interaction risks to be discharged through application of the tiered approach, especially when co-medications cannot be excluded in the desired patient population.

Using PBPK models to investigate drug interactions for oral or intravenous drugs is common practice and PBPK models can be built in SimCYP®, a commercially available PBPK software package and a proven methodology for assessing DDIs

DMD Fast Forward. Published on February 2, 2020 as DOI: 10.1124/dmd.119.089003
This article has not been copyedited and formatted. The final version may differ from this version.

(Shebley et al., 2018). Herein we describe a simple adaptation in SimCyp which enables an inhalation PBPK to model to be built and used to investigate drug interactions. To the authors knowledge an inhalation PBPK model has not previously been published for this purpose. Prior to developing and running prospective simulations with nemiralisib, the model was qualified using inhaled vilanterol, a CYP3A4 substrate with a published CYP3A4 clinical drug interaction study (Kempsford et al., 2013). The qualified PBPK model was then used to simulate the drug interactions as a victim following co-administration of strong and moderate CYP3A4 inhibitors such as clarithromycin and erythromycin (FDA 2006) on nemiralisib exposure) or as a perpetrator (e.g. influence of nemiralisib on exposure to sensitive narrow therapeutic index CYP3A4 substrates such as theophylline (Tjia et al., 1996).

This paper presents the results of an integrated strategy for assessing the DDI risk for inhaled nemiralisib using in vitro, clinical and in silico approaches which considered both victim and perpetrator risks for both drug transporters as well as CYP enzymes.

Materials and methods

Materials

Nemiralisib (Bis(6-(1*H*-indol-4-yl)-4-(5-{[4-(propan-2-yl)piperazin-1-yl]methyl}-1,3-oxazol-2-yl)-1*H*-indazole) succinate) was supplied as a solid by GlaxoSmithKline (GSK) Chemical Registry (Stevenage, UK). The purity of the material was > 95% with a molecular weight of the bis succinate salt of 999.2. Glucose-6-phosphate, glucose-6-phosphate dehydrogenase and β-nicotinamide adenine dinucleotide phosphate (NADP+) were supplied by Sigma Chemical Company, St. Louis, USA or Corning Life Sciences, Woburn, MA, USA Benzylnirvanol, sulphaphenazole,

DMD Fast Forward. Published on February 2, 2020 as DOI: 10.1124/dmd.119.089003
This article has not been copyedited and formatted. The final version may differ from this version.

furafylline, quinidine, digoxin, verapamil, estradiol glucuronide, rifampicin, cyclosporin A, p-Aminohippuric acid (PAH), probenecid, cimetidine, estrone sulfate, phenacetin, diclofenac (sodium salt), α-naphthoflavone, furafylline, tamoxifen (citrate salt), Thio-TEPA, quercetin, S-fluoxetine, testosterone, nifedipine and paroxetine hydrochloride were obtained from Sigma Chemical Company, St. Louis, USA. Montelukast and tienilic acid were obtained from Cayman Chemical Company, MI, USA. Efavirenz, S-mephenytoin, benzylnirvanol, R-bufuralol hydrochloride, midazolam and gemfibrozil hydrochloride were supplied by Toronto Research Chemicals Inc., Toronto, Ontario, Canada. Amadiaquine dihydrochloride dihydrate was supplied by Fluka Chemicals, St. Louis, USA. Nicotinamide adenine dinucleotide phosphate hydrate (NADPH) was supplied by MP Biomedical, Santa Ana, CA, USA. Azamulin was supplied by the GSK compound bank, GSK, Harlow, UK or Corning Life Sciences, Woburn, MA, USA.

^{3}H Digoxin, ^{14}C Mannitol, ^{3}H Prazosin, ^{3}H Estradiol 17β-D-glucuronide (E2G) and ^{3}H Estrone sulfate (ES) were obtained from PerkinElmer Inc. MA, USA. ^{3}H PAH was obtained from American Radiolabeled Chemicals, MO, USA, Ko143 from Biotechne. and ^{14}C metformin from Curachem, Korea.

Pooled human liver microsomes (HLMs) prepared from a mixed gender pool of 150 or 200 donors were obtained from Corning®, Woburn, MA, USA or Xenotech LLC, Lenexa, KS, USA, respectively. Human lung microsomes (HLuMs) prepared from mixed gender pools of 10 human non-smoker or smoker lungs (BioIVT, Baltimore, MD, USA). Supersomes™, containing individually over-expressed human CYP enzymes, derived from baculovirus infected insect cells, and control Supersomes™ (lacking any native human CYP activity) were obtained from BD Gentest, Woburn, MA, USA. Supersomes™ expressing CYP2C8, CYP2C9, CYP2C19, CYP3A4,

DMD Fast Forward. Published on February 2, 2020 as DOI: 10.1124/dmd.119.089003
This article has not been copyedited and formatted. The final version may differ from this version.

CYP2A6, CYP2B6, CYP2E1, CYP2J2 and CYP3A5 co-expressed CYP reductase and cytochrome b_5, while Supersomes™ expressing CYP1A2, CYP2D6 and CYP1A1 co-expressed CYP reductase only. Bactosomes expressing CYP2A13 with co-expressed CYP reductase in Escherichia coli were obtained from Cypex Ltd, Dundee, Scotland, UK. Supersomes™ and Bactosomes will be collectively referred to as recombinant CYP enzymes (rCYP).

All other chemicals used in these investigations were reagent grade or higher and were obtained from standard commercial suppliers.

Study conduct of in vitro assays and assessment of risk

The following work was conducted separate to the clinical drug interaction study: CYP and transporter phenotyping; CYP and transporter inhibition work; and development and application of the PBPK and mechanistic models. All of the work is reported in signed management approved GSK reports which are stored and available in GSK systems.

In vitro investigation of human oxidative enzymology of nemiralisib

The human CYP enzymes responsible for the oxidative metabolism of nemiralisib were investigated using a combination of in vitro incubation approaches; in HLMs and HLuM with and without the presence of selective CYP inhibitors and using recombinant CYP enzymes. Incubation times, protein concentration and cytochrome P450 content were predetermined from initial incubations to establish linear conditions.

Duplicate nemiralisib incubations were performed with pooled HLMs (30 min) and pooled HLuMs (120 min) in a shaking water bath. Each incubation contained 0.5 µM (or 5 µM, data on file) nemiralisib, potassium phosphate buffer (50 mM, pH 7.4) and either 0.5 mg/mL or 2 mg/mL microsomal protein in the liver or lung microsome

incubations, respectively. Reactions were initiated by the addition of cofactor solution (an NADPH regenerating system containing a final concentration of approximately 0.44 mM NADP+, 5.5 mM glucose-6-phosphate and 1.2 units/mL glucose-6-phosphate dehydrogenase). Reactions were terminated by adding a volume of acetonitrile equal to the incubation volume. Inhibition of nemiralisib cytochrome P450 metabolism was investigated using HLMs using a method previously described (Lawrence et al., 2014). Incubations (0.5 µM nemiralisib, 0.5 mg/mL microsomal protein, 30 min) were conducted in duplicate in the presence and absence of the following selective CYP inhibitors: azamulin (CYP3A4), sulphaphenazole (CYP2C19), quinidine (CYP2D6), montelukast (CYP2C8), benzylnirvanol (CYP2C19) or furafylline (CYP1A2).

Nemiralisib incubations were also performed with a range of human rCYPs containing over-expressed individual CYP enzymes. Each incubation contained 0.5 µM nemiralisib; an appropriate volume of potassium phosphate buffer (50 mM, pH 7.4) and rCYP at one of the following concentrations (and incubation times): 300 pmol/mL (CYP1A2, CYP2A6, CYP2A13, CYP2B6, CYP2C9, CYP2C19, CYP2D6 or CYP2E1 (120 mins)); 75 pmol/mL (CYP1A1 or CYP2C8 (60 mins)); 50 pmol/mL CYP2J2 (60 mins); 25 pmol/mL (CYP3A4, CYP3A5 (30 mins)). Reactions were initiated and terminated in a similar manner to that described above.

Control incubations were performed in the absence of each of, microsomes, Cofactor, rCYP enzymes and nemiralisib. Following centrifugation of incubations at 13,000g for 3 minutes, the supernatants were analyzed by ultra performance liquid chromatography liquid chromatography - mass spectrometry (UPLC-LC/MS^n) detection. Quantification was conducted on UV peaks over 3% region of interest (ROI) integrated peaks only. Quantitation by UV detection was preferred over MS for

DMD Fast Forward. Published on February 2, 2020 as DOI: 10.1124/dmd.119.089003
This article has not been copyedited and formatted. The final version may differ from this version.

a number of reasons: nemiralisib and its metabolites have strong chromophores; metabolite standard was only available for one metabolite (M1); and preliminary work (not shown) indicated better linearity for UV response compared with MS response. Drug-related UV peaks were identified following comparison of control and test incubations. Each drug-related UV peak was then integrated and expressed as % region of interest from which a concentration was calculated with reference to the nominal target incubation concentration. At both concentrations (0.5 and 5µM) the main metabolites were quantifiable.

Metabolite structural assignments were based on UPLC-LC/MS^n and/or comparisons of metabolite identification by UPLC-LC/MS^n from previous work and authentic metabolites, where available.

In vitro evaluation of nemiralisib as an inhibitor of cytochrome P450 (CYP) enzymes: 1A2, 2B6, 2C8, 2C9, 2C19, 2D6 and 3A4

Incubation conditions for the assay of the enzyme activities: CYP1A2, 2B6, 2C8, 2C9, 2C19, 2D6 and CYP3A4 are shown in Supplementary Table S3. All incubations were performed at the K_m previously determined for each probe substrate (concentration of substrate that leads to half-maximal velocity), and incubation times and HLM concentrations used reflect linear rate incubation conditions for the probe substrate reactions. For both reversible inhibition and metabolism dependent inhibition (MDI) experiments, positive control incubations (replacing nemiralisib) with an appropriate concentration range of a known reversible or metabolism-dependent CYP inhibitor, and control incubations without inhibitor (containing 1 % v/v methanol only) were performed for all CYPs. All samples were centrifuged to compress the precipitated protein into a pellet and supernatants were monitored for probe substrate metabolite formation using LC/MS-MS. Further analytical details and

DMD Fast Forward. Published on February 2, 2020 as DOI: 10.1124/dmd.119.089003
This article has not been copyedited and formatted. The final version may differ from this version.

details of internal standards are shown in Supplementary Table S4. Rates of metabolite production at each concentration of nemiralisib or positive control inhibitor were expressed as a percentage of the mean uninhibited control rate for each assay and half maximal inhibitory concentration (IC_{50}) curves fitted from a log-transformation of inhibitor concentration vs. percentage remaining metabolite formation at each inhibitor concentration. MDI was inferred from a decrease in IC_{50} on pre-incubation in the presence vs. the absence of NADPH.

Reversible and metabolism-dependent inhibition (MDI) of CYP1A2, 2B6, 2C8, 2C9, 2C19 and CYP2D6

Pre-incubation reaction mixtures contained incubation mix (100 mM sodium buffer, pH 7.4 and HLM) and an aliquot of nemiralisib solution in methanol, with and without NADPH (1 mM final concentration) for MDI and reversible inhibition, respectively. Triplicate incubations were prepared with each concentration of nemiralisib. After pre-incubation (37°C, 30 min), probe substrate was added to the reversible inhibition pre-incubation samples prior to the immediate initiation of reaction by addition of NADPH (1 mM final concentration). After pre-incubation (37°C, 30 min) including NADPH, reactions were initiated in the MDI pre-incubation samples by addition of probe substrate. Final incubation concentrations of nemiralisib were 0.0875, 0.292, 0.972, 3.24, 10.8, 36, and 120 µM. Reactions were terminated after the appropriate incubation time by the addition of 100 µL of acetonitrile containing a suitable internal standard.

Reversible and metabolism dependent inhibition of CYP3A4

Pre-incubation reaction mixtures for CYP3A4 contained 0, 0.03, 0.1, 0.3, 1.0, 3.0, 10 and 30 µM of nemiralisib, and microsomal protein in 100 mM potassium phosphate buffer (pH 7.4), with and without an NADPH-regenerating system (1.3 mM NADP+,

DMD Fast Forward. Published on February 2, 2020 as DOI: 10.1124/dmd.119.089003
This article has not been copyedited and formatted. The final version may differ from this version.

3.3 mM glucose-6-phosphate, 0.4 U/mL glucose-6-phosphate dehydrogenase, and 3.3 mM magnesium chloride). After 30 min of pre-incubation time at 37°C, each pre-incubation reaction was diluted 1 in 10 by transferring an aliquot into a pre-warmed secondary reaction mixture containing NADPH-regenerating system and one concentration of probe substrate in 100 mM potassium phosphate buffer (pH 7.4). Reactions were incubated at 37°C for an appropriate incubation time, stopped by addition of 100 µL 0.1% formic acid in acetonitrile containing a suitable internal standard and placed on ice.

Determination of the MDI kinetics

Inactivation incubations with nemiralisib were performed in a 96-well plate heated at 37°C. Pre-incubation mixtures contained 100 mM sodium or potassium phosphate buffer, pH 7.4 (CYP1A2 and 2B6, and CYP3A4, respectively), HLM and various concentrations of nemiralisib solution in methanol. Inactivation reactions were initiated by the addition of NADPH (either as an aliquot of 10 mM NADPH (CYP1A2 and 2B6) or as an NADPH-regenerating system consisting of 1.3 mM NADP+, 3.3 mM glucose-6-phosphate, 0.4 U/mL glucose-6-phosphate dehydrogenase, and 3.3 mM magnesium chloride (CYP3A4)). Final inactivation incubation concentrations of nemiralisib were 1.88, 3.75, 7.5, 15, 30, 60, and 120 µM for CYP1A2 and CYP2B6, and 0, 0.1, 0.3, 1.0, 3.0, 10, 30 and 100 µM for CYP3A4. At multiple inactivation time points, aliquots of the inactivation reaction mixtures were withdrawn and diluted into a pre-warmed (37°C) CYP-specific activity assay incubation system containing NADPH or an NADPH regenerating system, and the appropriate probes substrate in phosphate buffer (100 mM, pH 7.4). This activity assay mixture was incubated for an additional CYP-specific incubation time. Reactions were terminated by the addition of stop solution containing an appropriate internal standard. Incubation details can

DMD Fast Forward. Published on February 2, 2020 as DOI: 10.1124/dmd.119.089003
This article has not been copyedited and formatted. The final version may differ from this version.

be found in Supplementary Table S5. Positive control incubations (replacing nemiralisib with appropriate concentrations of furafylline for CYP1A2, thio-TEPA for CYP2B6 or azamulin for CYP3A4) and control incubations without inhibitor (containing 1% v/v methanol only) were also performed.

All samples were centrifuged to compress the precipitated protein into a pellet and supernatants were monitored for probe substrate metabolite formation using LC/MS-MS. The natural logarithm of the residual activity (corrected for loss of activity observed over time in the absence of nemiralisib) was plotted against the pre-incubation time for each concentration of nemiralisib. The first-order rate constant for inactivation was estimated from the linear portion of the curves and inactivation parameters (nemiralisib (inactivator) concentration required to achieve half-maximal inactivation rate (K_i) and maximal rate constant of inactivation (k_{inact}) were determined using non-linear regression analysis of the generated apparent rate constants at each concentration of nemiralisib.

Inhibition of transporters by nemiralisib

An in vitro study to determine the inhibitory potency of nemiralisib against P-gp, breast cancer resistance protein (BCRP), organic anion transporting polypeptide 1B1 (OATP1B1), OATP1B3, OAT1, OAT3, organic cation transporter 2 (OCT2), multidrug and toxin extrusion 1 (MATE1) and MATE2-K, using porcine kidney epithelial cell line (LLC-PK1 cells) stably expressing P-gp or BCRP and human embryonic kidney mammalian (HEK293) cells stably expressing OATP1B1, OATP1B3, OAT1, OAT3, OCT2, MATE1 or MATE2-K, and control cells was conducted. Cell monolayers were pre-incubated at 37°C with buffer alone and buffer containing nemiralisib (0.0003 - 10 µM for P-gp and BCRP, and 0.001 - 30 µM for OATP1B1, OATP1B3, OAT1, OAT3, OCT2, MATE1 and MATE2-K). After pre-incubation was completed, cells were

DMD Fast Forward. Published on February 2, 2020 as DOI: 10.1124/dmd.119.089003
This article has not been copyedited and formatted. The final version may differ from this version.

incubated in triplicate with buffer containing probe substrate, 1 µM [^{3}H]digoxin (P-gp), 0.01 µM [^{3}H]prazosin (BCRP), 0.05 µM [^{3}H]E2G (OATP1B1 and OATP1B3), 1 µM [^{3}H]PAH (OAT1), 0.05 µM [^{3}H]ES (OAT3) or 10 µM [^{14}C]metformin (OCT2, MATE1 and MATE2-K) and appropriate amount of nemiralisib. Verapamil (P-gp), Ko143 (BCRP), cyclosporine A (OATP1B1 and OATP1B3), probenecid (OAT1 and OAT3) and cimetidine (OCT2, MATE1 and MATE2-K) were included as positive control inhibitors. Further details of the experimental conditions can be found in Supplementary Table S6.

Clinical drug-drug interaction study design, subjects and assessments

Study design

The DDI study was a phase I, single-center, open-label, crossover study in healthy male subjects conducted by Quintiles (Kansas, United States) between January 2018 and March 2018 (GSK study number 206874; ClinicalTrials.gov registration number NCT03398421). The study was approved by the Chesapeake Institutional Review Board (Maryland, United States), adhered to the Declaration of Helsinki and written informed consent was obtained from each subject.

All subjects had a screening visit followed by two treatment periods with a 14 day washout period between treatments (Figure 1). Nemiralisib hemisuccinate salt was blended with lactose and magnesium stearate and packed in foil blisters containing 100 µg free base per blister in the Ellipta device. In treatment period 1, subjects received a single oral-inhaled dose of nemiralisib, 100 µg via the Ellipta inhaler on Day 1, and blood samples for pharmacokinetic (PK) analysis were collected up to 120 h post-dose. In treatment period 2, subjects received 2 oral capsules of itraconazole (200 mg total dose; supplied by Amneal Pharmaceuticals LLC, Bridgewater, New Jersey; manufactured by Amneal Pharmaceuticals Pvt. Ltd.,

DMD Fast Forward. Published on February 2, 2020 as DOI: 10.1124/dmd.119.089003
This article has not been copyedited and formatted. The final version may differ from this version.

Ahmedabad, India) daily from day 1 to 10 and a single oral-inhaled dose of nemiralisib 100 µg on Day 5, 1 h after itraconazole. Blood samples for PK analysis were collected on Day 1 (pre-dose and up to 12 h post-dose) and Day 5 (pre-dose and up to 24 h post-dose) for itraconazole and hydoxy-itraconazole, and on Days 5 (up to 144 h post-dose) for nemiralisib. This design was based on that reported by Ke et al (2014).

Subjects

Healthy male subjects who were aged from 18-75 years, weighed 50 kg or more, had a body mass index (BMI) of 18-35 kg/m^2 and normal spirometry (both forced expiratory volume in 1 second and forced vital capacity ≥80% of predicted) were included. Subjects with any clinically significant disease (including abnormal liver function), abnormal blood pressure, a history of alcohol or drug abuse and current smokers (or smoking history within previous 6 months and a total pack year history of >5 pack years) were excluded. Full eligibility criteria details are given on ClinicalTrials.gov (NCT03398421).

Pharmacokinetic assessments

Blood samples were collected into tripotassium ethylenediaminetetraacetic acid tubes, centrifuged and plasma was harvested and stored at -20°C prior to shipment for analysis. Plasma samples were analyzed for nemiralisib (GSK, Philadelphia, USA) using a validated analytical method based on protein precipitation using acetonitrile containing [$^2H_7$] nemiralisib as an internal standard, followed by ultra high performance liquid chromatography and TurboIonSpray™ tandem mass spectrometric detection (UHPLC-MS/MS analysis). The lower limit of quantification (LLQ) was 5 pg/mL using a 50 µL aliquot of human plasma with a higher limit of quantification (HLQ) of 1000 pg/mL. Typically, a 10 µL aliquot of extracted sample

DMD Fast Forward. Published on February 2, 2020 as DOI: 10.1124/dmd.119.089003
This article has not been copyedited and formatted. The final version may differ from this version.

was injected onto a LC system consisting of a 50 x 2.1 mm i.d. Waters Acquity BEH C18 1.7µm column and a Waters Acquity UPLC system. Mobile phases of 10 mM ammonium bicarbonate (pH 9) and acetonitrile at a flow rate of 0.8 mL/min and a column temperature of 60°C were used to elute Nemiralisib at a typical retention time of 0.9 minutes. Analysis for itraconazole and hydroxy-itraconazole (Covance Laboratories Limited, Harrogate, UK) was performed using an analytical method based on solid phase extraction, followed by LC/MS/MS analysis. The LLQ was 2 ng/mL using a 100 µL aliquot of EDTA plasma. The HLQ was 1000 ng/mL.

Safety assessments

In treatment period 1, vital signs and 12-lead electrocardiograms (ECGs) were measured pre-nemiralisib dose on Day 1 and at Day 6 before discharge. In treatment period 2, vital signs/ECGs were measured on Day 1 (pre-dose and 3 h post-dose (ECG only) and pre-dose on Days 2, 4, 6, 8 and 10. Routine laboratory tests were performed at Day -1 for each treatment period and on Day 6 (treatment period 1) and Day 10 (treatment period 2). In treatment period 2, additional samples for clinical chemistry were collected pre-dose on Days 2, 4, 6 and 8. Adverse events were monitored throughout the study.

Static mechanistic evaluation for nemiralisib effect on theophylline exposure

Theophylline is an oral bronchodilator commonly prescribed in the treatment of asthma and COPD. In vitro studies have shown CYP1A2 to be the major enzyme responsible for the metabolism of theophylline with minor contributions from other CYP enzymes including CYP3A4 (Tjia et al., 1996). To allow safe dosing of theophylline with nemiralisib, a mechanistic-based drug interaction assessment was conducted using the CYP3A4 inactivation kinetic parameters determined for nemiralisib.

DMD Fast Forward. Published on February 2, 2020 as DOI: 10.1124/dmd.119.089003
This article has not been copyedited and formatted. The final version may differ from this version.

The static mechanistic model, as described by the FDA (2017b), incorporates irreversible inhibition and contribution of intestinal metabolism for CYP3A4 substrates, which were applied to estimate the magnitude of increase in theophylline exposure (area under the concentration time curve (AUC)) when co-administered with nemiralisib. As a conservative approach, the fraction of liver metabolism of theophylline by CYP3A4 was set to 1. Intestinal metabolism of theophylline was deemed negligible based on the minimal difference in AUC ratios observed in clinical intravenous and oral drug interaction studies with Verapamil (Stringer et al., 1992; Sirmans, 1988).

Physiologically based pharmacokinetic (PBPK) modelling to predict nemiralisib DDI

PBPK platform qualification

A clinical DDI study between vilanterol and ketoconazole was simulated to qualify the use of the PBPK platform Simcyp® (Version 17, Release 1, SimCYP Ltd, Sheffield, UK). Like nemiralisib, vilanterol is an inhaled drug with metabolism via CYP3A4 the main clearance route in humans, and so was deemed suitable for qualification of the prediction of DDI between an inhaled CYP3A4 substrate and potent CYP3A4 inhibitor to regulatory expectations. A clinical study following co-administration of repeat once-daily 400 mg of ketoconazole and single dose 25 µg of inhaled vilanterol resulted in an average 1.9-fold increase in vilanterol systemic exposure (AUC) but negligible change in its maximum observed plasma concentration (C_{max}). A PBPK model incorporating the mechanistic clearance pathway was built for vilanterol using Simcyp® (a listing of model parameters is shown in Table S7), and validated with actual clinical studies at 100 and 25 µg

DMD Fast Forward. Published on February 2, 2020 as DOI: 10.1124/dmd.119.089003
This article has not been copyedited and formatted. The final version may differ from this version.

inhaled vilanterol. Once validated, a DDI simulation was then run between vilanterol and ketoconazole (in-built file within SimCYP®) and the extent of simulated DDI was compared with the actual clinical DDI study (Kempsford et al., 2013).

Nemiralisib inhalation PBPK model development and qualification

An intravenous mechanistic PBPK model was developed initially using the SimCYP® ADME (absorption, distribution, metabolism and excretion) simulator. To develop the nemiralisib compound file, measured physicochemical properties (e.g. molecular weight, octanol:water partition coefficient, blood to plasma ratio and plasma protein binding) were entered into the Simcyp® software along with mean observed volume of distribution and intravenous clearance, using data from a previous clinical study (Harrell et al., 2019). A full listing of the nemiralisib model parameters are shown in Table S8. Simulations were then conducted to predict and compare nemiralisib plasma exposure (AUC) and half-life after a 10 µg (nominal dose) 15-min intravenous infusion. SimCYP-simulated dosing regimens for studied scenarios were performed according to their actual clinical trial study design and delivered doses (Wilson et al., 2019; Harrell et al., 2019). To complete the intravenous PBPK model, the in vivo clearance was converted to enzymes kinetics using the retrograde calculator within SimCYPv17. The mean CYP3A4 percentage contribution used for the calculator was determined in vitro from recombinant expressed enzymes and HLM. The remaining non-CYP3A4 clearance routes were combined under additional HLM clearance. The intravenous PBPK model was converted to an oral PBPK model using the first order oral absorption model within SimCYP®, and the model was qualified by comparing simulated fraction absorbed and bioavailability with observed following a single oral dose of 800 µg nemiralisib (Harrell et al., 2019). The final stage of the PBPK model build utilized the parameter estimation module to optimize

DMD Fast Forward. Published on February 2, 2020 as DOI: 10.1124/dmd.119.089003
This article has not been copyedited and formatted. The final version may differ from this version.

the rate of absorption to the lung after an inhaled dose, using AUC data after a 1000 ug dose (Harrell et al., 2019). The estimate of fraction absorbed in the lung was obtained from dosimetry data generated using a stand-alone computational model, Multiple-Path Particle Dosimetry (MPPD) v2.92.5 (Applied Research Associates, Raleigh, North Carolina, US).

The PBPK inhaled model was further qualified by comparing simulated data with plasma exposures of nemiralisib after a 500 µg dose (Wilson et al., 2019) and 100 µg dose (clinical DDI study).

A retrospective simulation of the clinical DDI study between nemiralisib and itraconazole (NCT03398421 as described herein) was performed to evaluate whether SimCYP® could accurately simulate this interaction based on the nemiralisib profile described.

Nemiralisib inhalation PBPK model application

Nemiralisib inhaled PBPK model victim simulations

To predict the effect of the macrolide inhibitors, clarithromycin and erythromycin, on the exposure of nemiralisib, drug interaction simulations were conducted using the clinical study designs from Gorski et al (1998) and Olkkola et al (1994).

Nemiralisib inhaled PBPK model perpetrator simulations

To predict the effect of nemiralisib on the exposure of the sensitive CYP3A4 index substrate midazolam, a typical perpetrator drug clinical dosing regimen was simulated. To fully elucidate the effect of nemiralisib, repeat dose exposure profiles were simulated to steady state.

Statistical analysis

For the in vitro investigation, statistical analysis was limited to the calculation of means, where appropriate (Excel, Microsoft™, Redmond, WA). Metabolite peaks

DMD Fast Forward. Published on February 2, 2020 as DOI: 10.1124/dmd.119.089003
This article has not been copyedited and formatted. The final version may differ from this version.

were quantified by fractional conversion from parent observed on the chromatograms by UV area detection.

The sample size for the clinical DDI study was primarily based on feasibility. It was estimated, however, that with 16 subjects providing the relevant PK parameter data, the upper bound of the 90% confidence interval (CI) would be within approximately 22% of the point estimate and the lower bound within 18% for $AUC_{0\text{-}inf}$. For C_{max} the upper bound of the 90% CI was estimated to be within approximately 23% of the point estimate and the lower bound within 19%. Plasma concentration time data for nemiralisib and for itraconazole were analyzed by non-compartmental methods with WinNonlin Version 7.0, using the actual sampling times recorded during the study for derivation of PK parameters. For the PBPK modelling simulations, the statistical assessment for each set of data was performed by comparing the distribution of the simulated individuals to the distribution of the observed data.

Application of tiered approach guided by FDA 2017

A tiered approach to investigating DDI, as described in FDA 2017b, was followed for nemiralisib. FDA recommends an initial investigation using basic equations which essentially compare enzyme potency to free (unbound) drug systemic exposure (referred to as $I_{max,u}$) to generate values for R_1 (reversible inhibition), R_2 (metabolism dependent inhibition) and R_1 gut (reversible inhibition at the gut). Further details can be found in Supplementary Table S1. Further investigations are required if parameter thresholds are exceeded following the application of these equations (R_1 ≤1.02, R_2 ≤1.25 or R_1gut ≤11). As a result, the determination of $I_{max,u}$ is an important component of any perpetrator drug interaction potential consideration. For nemiralisib, $I_{max,u}$ was calculated assuming a pharmacological dose of 750 µg (delivered as a dry powder in the intended clinical device by the inhalation route).

DMD Fast Forward. Published on February 2, 2020 as DOI: 10.1124/dmd.119.089003
This article has not been copyedited and formatted. The final version may differ from this version.

The steady state plasma C_{max} was assumed to be 3.6 ng/mL calculated from measured single dose data (Wilson et al., 2019), multiplied by an accumulation ratio measured following repeated administrations (Wilson et al., 2018) and it was assumed that the free fraction in plasma was 0.021 (2.1%) (unpublished data). As would be expected for a low dose inhalation molecule, $I_{max,u}$ was extremely low (calculated as 0.2 nM, using a free base molecular weight of 441).

Results

In vitro oxidative enzymology of nemiralisib

Incubation of 0.5 µM nemiralisib with the range of rCYP enzymes investigated together with the scaling of the expressed metabolite production to reflect amounts present in HLMs, indicated that the P450 enzyme predominantly responsible for metabolism of nemiralisib was CYP3A4 (95% contribution to metabolism; Table 1). CYP1A2, 2C8, 2C9, 2C19 and 2D6 collectively contributed to ~5% of hepatic metabolism of nemiralisib. Following the incubation of 0.5 µM nemiralisib with HLMs and selective CYP inhibitors, the production of M1 (a major N-dealkylated metabolite) was predominantly inhibited by the CYP3A4 inhibitor azamulin (55%), followed by the CYP2C8 inhibitor montelukast (15%). As CYP3A4 percent contribution ranged from 55-95%, a mean contribution of ~75% CYP3A4 metabolism was used in the PBPK model. Nemiralisib was not metabolized by HLuMs. Due to the predominant contribution of CYP3A4 metabolism of nemiralisib observed in vitro in liver it was not unexpected that no metabolism in HLuMs was seen, where CYP3A4 expression in lung is negligible (Somers et al, 2007).

In vitro inhibition of CYPs in HLMs by nemiralisib.

Nemiralisib inhibited the probe marker activity of CYP1A2, 2B6, 2C8, 2C9, 2C19, 2D6 and 3A4 in HLMs, with IC_{50} values of 58.2, 44.4, 26.4, 13.6, 12.0, 7.94 and >3

DMD Fast Forward. Published on February 2, 2020 as DOI: 10.1124/dmd.119.089003
This article has not been copyedited and formatted. The final version may differ from this version.

µM, respectively. Nemiralisib was an MDI of CYP1A2, CYP2B6 and CYP3A4 with a decrease in IC_{50} value following a 30-minute pre-incubation with cofactor of 2.7, 1.9-fold and >7.9 (highest fold change observed), respectively. MDI kinetic evaluation showed that nemiralisib was not an inactivator of CYP1A2. It was, however, an apparent inactivator of CYP2B6 and 3A4 with a k_{inact} of 0.014 and 0.034 min-1, and a K_i of 2.0 and 4.2µM, respectively (Table 2). The potential for increased exposure of the CYP2B6 substrate Bupropion, on co-administration with nemiralisib, was estimated using static mechanistic models. When surrogates of nemiralisib concentration were corrected for plasma protein binding, the maximum extrapolated drug interaction was a 1.0-fold change for bupropion, indicative of no anticipated change of their exposure due to CYP inhibition when co-administered with nemiralisib. A parallel assessment with the CYP3A4 probe substrate midazolam suggested that nemiralisib may elicit a potential GI- mediated clinical drug-drug interaction. To further confirm and quantify this risk, the PBPK model described herein was used to simulate nemiralisib dynamic profiles with midazolam.

In vitro inhibition of transporters by nemiralisib.

Nemiralisib, at a concentration of 30 µM, decreased the P-gp-mediated transport of digoxin by 69% and inhibited BCRP-mediated transport of by Prazosin by 74%. Nemiralisib (30µM) inhibited OATP1B1 and 1B3-mediated transport of estradiol glucuronide transport by 89 and 85%, with resulting IC_{50} values 3.03 and 1.76, respectively. Nemiralisib reduced transport of metformin via OCT2, MATE1 and MATE2-K by 98, 99 and 100%, leading to sub-micromolar IC_{50} values (0.381, 0.0260 and 0.0545 µM, respectively). Nemiralisib did not inhibit drug transporters: OAT1 and OAT3 at concentrations up to 30 µM. The inhibitory effects of nemiralisib and positive control inhibitors are summarized in Supplementary Table S9. Unpublished

DMD Fast Forward. Published on February 2, 2020 as DOI: 10.1124/dmd.119.089003
This article has not been copyedited and formatted. The final version may differ from this version.

GSK data has indicated that nemiralisib is a substrate of P-gp and BCRP but not a substrate for OAT1B1, OAT1B3 and OCT1.

Clinical drug-drug interaction study

Demographic and baseline characteristics

Twenty healthy male subjects were enrolled and completed the study. Their mean (SD) age was 36 (12) years and BMI was 28 (3.9) kg/m^2.

Pharmacokinetic data

The plasma PK profiles of inhaled nemiralisib were visually similar following single dose administration of nemiralisib and administration of nemiralisib with itraconazole, characterized by fast absorption (time to maximum observed plasma concentration (t_{max}) of 0.7 h and 0.9 h, respectively) and C_{max} occurring up to two hours post-dose, followed by a rapid, then slower, decline in plasma concentrations (Figure 2). Nemiralisib plasma concentrations were higher following nemiralisib dosed with itraconazole compared with nemiralisib alone. The adjusted geometric LS mean ratios for $AUC_{0\text{-}inf}$ and C_{max} demonstrated, respectively, that the systemic exposure of nemiralisib was 101% greater (an increase of 2.01-fold) and maximum plasma concentration was 20% lower following co-administration versus nemiralisib alone (Table 3). The 90% CIs for the geometric LS means ratios fell entirely outside the standard equivalence limits of 0.80 to 1.25 for these parameters indicating that itraconazole had a clinically relevant effect on the systemic exposure of nemiralisib. Plasma exposures for itraconazole and hydroxy-itraconazole are shown in Supplementary Table S10.

Safety

One adverse event (AE) of headache was reported following treatment with nemiralisib alone; AEs of upper respiratory tract infection (2 events) and one each of

DMD Fast Forward. Published on February 2, 2020 as DOI: 10.1124/dmd.119.089003
This article has not been copyedited and formatted. The final version may differ from this version.

hypoacusis and dry eye were reported in the nemiralisib with itraconazole arm. No serious AEs or AEs leading to withdrawal were reported. The event of hypoacusis was judged as related to itraconazole by the investigator, was mild in intensity and resolved after two days. There were no clinically significant changes in other safety parameters.

Static mechanistic evaluation for nemiralisib effect on theophylline exposure

The static mechanistic model to evaluate the impact of nemiralisib on theophylline, showed that at clinically relevant concentrations, nemiralisib would not alter the systemic exposure of theophylline with the highest potential fold change for theophylline exposure predicted to be <1.2 fold.

Physiologically based pharmacokinetic modelling data

PBPK software qualification

Simulated PK parameters for inhaled vilanterol 100 µg or 25 µg were within the bioequivalence limit of quantification which qualified the PBPK model built for vilanterol using Simcyp® (Supplementary Table S11). Similarly, the AUC and C_{max} ratios in the DDI simulations with ketoconazole were predicted within the bioequivalence limits (Supplementary Table S12). The observed geometric mean C_{max} and AUC ratio for vilanterol-ketoconazole DDI were 0.90 and 1.90 respectively which compare well with the simulated C_{max} and AUC ratios of 1.10 and 1.72 respectively.

PBPK model qualification

The SimCYP®-simulated and observed plasma concentration time curves for nemiralisib following IV 10 µg, oral 800 µg and inhaled 1000 µg administration are shown in Figure 3. Simulated PK parameters were within acceptable bioequivalence limits of those observed clinically for all PBPK models (Supplementary Table S13). In

DMD Fast Forward. Published on February 2, 2020 as DOI: 10.1124/dmd.119.089003
This article has not been copyedited and formatted. The final version may differ from this version.

addition, the mean SimCYP simulated oral bioavailability of 35% was within the range observed clinically following an 800 µg oral dose: 33.7% - 36.5% (Harrell et al., 2019). The in silico MPPD simulations predicted that 54% of the 1000 µg (540 µg) to be deposited in the lung. It is assumed that all of this drug deposited in the lung is absorbed. Further qualification of the inhaled nemiralisib model using simulated PK parameters to predict exposure after single inhaled doses of 500 µg and 100 µg also demonstrated data within acceptable bioequivalence limits (data not shown).

Finally, the retrospective simulation of the clinical DDI study between nemiralisib and itraconazole showed good agreement between the simulated and observed data ($AUC_{0\text{-}inf}$ ratio 2.3 and 2.0, respectively; Table 4).

PBPK model application

The PBPK SimCYP® model predicted a weak drug interaction following co-administration of clarithromycin and erythromycin (simulated $AUC_{0\text{-}inf}$ ratio of 1.71 and 1.67, respectively; Table 5). The simulated midazolam drug interaction study to assess the impact of nemiralisib on the exposure of sensitive CYP3A4 substrates, showed no change in the exposure of midazolam with steady-state dosing of nemiralisib 750 µg once daily. A sensitivity analysis indicated that nemiralisib doses of greater than 100 times those used clinically would be needed to elicit a clinically relevant interaction with midazolam (Figure S1).

Discussion

According to FDA (2017b) moderate sensitive CYP3A4 substrates are drugs whose $AUC_{0\text{-}inf}$ values increase by 2- to 5- fold when co-administered with strong index CYP3A4 inhibitors such as itraconazole. The 2.01-fold increase in $AUC_{0\text{-}inf}$ for

DMD Fast Forward. Published on February 2, 2020 as DOI: 10.1124/dmd.119.089003
This article has not been copyedited and formatted. The final version may differ from this version.

nemiralisib when co-administered with itraconazole would therefore be classified as a moderate drug interaction, albeit at the very low end of this classification range. Importantly, the observed systemic exposure to itraconazole and its metabolite in the clinical study were in line with that observed following repeat doses of itraconazole at 200 mg once daily (Backman, 1998), confirming that, based on systemic exposure, adequate drug levels of itraconazole were achieved for maximal inhibition of CYP3A4. In comparison to the small fold changes to nemiralisib elicited by itraconazole, co-administration of itraconazole with midazolam (a sensitive CYP3A4 substrate) resulted in an 11-fold change in midazolam $AUC_{0\text{-}inf}$ (Olkkola et al.,1994), substantially higher than that observed for nemiralisib. It is important to be able to extrapolate changes in systemic exposure observed in clinical drug interaction studies, not only to other potential co-medications with increased or decreased potency, but also to different routes, doses, regimens or patient groups.

For this purpose, the PBPK platform Simcyp® was qualified for inhalation using a published victim drug interaction for inhaled vilanterol with ketoconazole (Kempsford et al., 2013) - the resultant simulated DDI for inhaled vilanterol were well within acceptable limits. In addition, the inhaled nemiralisib SimCYP® PBPK model also accurately predicted the PK exposures observed in the clinical DDI between nemiralisib and itraconazole, reported herein.

SimCYP® (version 17) does not have a specific inhalation application but additional drug inputs can be built into the PBPK model using the SimCYP® parameter estimation module which, simply, requires an amount of drug and a rate constant (modelled from previous clinical studies). In this case, the amount of drug deposited in the lung was determined using MPPD which is a sophisticated stand-alone tool to predict the total and regional human lung deposition from a given drug particle size

DMD Fast Forward. Published on February 2, 2020 as DOI: 10.1124/dmd.119.089003
This article has not been copyedited and formatted. The final version may differ from this version.

profile (Asgharian et al., 1999; Asgharian et al., 2006; Manojkumar et al., 2019). Other lung/inhalation models are nicely summarized by Borghardt et al (2015). Boger and Friden (2019), and Boger and Wigstrom (2018), describe multi-compartment inhaled PBPK models which mechanistically describe processes such as deposition, muco-ciliary clearance and dissolution. Andersen et al (2000), incorporated computational fluid dynamic models to estimate the flux of inhaled chemicals in animal nasal cavities. However, at the time, it was not possible to combine any of these sophisticated approaches directly with SimCYP® to investigate, drug interaction liability.

The inhaled nemiralisib PBPK model was used to model prospective simulations with other CYP3A4 inhibitors including with common co-medications in target patient populations. The $AUC_{0\text{-}inf}$ ratios of nemiralisib simulated by the PBPK model following co-administration with clarithromycin and erythromycin (1.71- and 1.67- fold respectively) would be classified as weak interactions (FDA 2017b) with resultant nemiralisib systemic exposures (both AUC and C_{max}) considerably lower than exposures at the No Adverse Effect Levels in animal toxicology studies (GSK unpublished data). Any small changes in nemiralisib exposure, because of CYP3A4 inhibition, were within the systemic overages calculated from long term animal studies and of negligible significance for human administrations of nemiralisib up to 750 µg. The clinical drug interaction study between nemiralisib and itraconazole and subsequent extrapolations using the PBPK model indicated that dosing restrictions with other strong CYP3A4 inhibitors, such as chronically administered macrolide antibiotics are not required. As a result, in our opinion, it was concluded that erythromycin and clarithromycin (common-comedications in a COPD or

DMD Fast Forward. Published on February 2, 2020 as DOI: 10.1124/dmd.119.089003
This article has not been copyedited and formatted. The final version may differ from this version.

bronchiectasis indication) could be safely co-administered with nemiralisib in any subsequent clinical trials.

Although itraconazole is also a potent P-gp inhibitor and nemiralisib is a P-gp substrate (data not shown), the clinical DDI study results do not demonstrate a significant P-gp interaction as a result of P-gp inhibition in the GI tract. Co-administration of nemiralisib with itraconazole did not increase nemiralisib C_{max} which would be expected for a relevant P-gp mediated interaction. Furthermore, inspection of time concentration profiles (Figure 2) shows the increase in nemiralisib AUC is driven by an increased elimination half-life in the inhibited state, which is consistent with a CYP3A4 interaction. Any clinically significant DDI between nemiralisib and P-gp inhibitors is unlikely since nemiralisib is high permeability (157 nm/s in cell monolayers – unpublished data) and is well absorbed in human (Harrell et al., 2019).

Using the tiered approach described in FDA (2017b), no further DDI investigations were required for CYP1A2, 2C8, 2C9, 2C19, or 2D6 (i.e. R_1 ≤1.02, R_2 ≤1.25 or R_1 gut ≤11) following the application of basic equations. The next tier of investigation (static mechanistic models) was, however, triggered for CYP3A4 and CYP2B6 where "R value" thresholds were exceeded for direct inhibition on the GI tract (CYP3A4) and MDI (CYP3A4 and CYP2B6). Static mechanistic models indicated no DDI risk associated with CYP2B6 but could not be used to discharge the CYP3A4 DDI perpetrator risks which, therefore, required escalation to the next tier of investigation involving the application of a PBPK model. Application of the inhaled nemiralisib PBPK model, developed and applied herein, indicated no risk of a CYP3A4 perpetrator DDI for nemiralisib. A sensitivity analysis using midazolam revealed that doses well in excess of likely nemiralisib clinical doses (approximately 100-fold)

DMD Fast Forward. Published on February 2, 2020 as DOI: 10.1124/dmd.119.089003
This article has not been copyedited and formatted. The final version may differ from this version.

would be required to elicit a significant drug interaction (≥1.25-fold) as a result of CYP3A4 metabolism-dependent inhibition. A specific investigation into the potential for a DDI between nemiralisib and theophylline, a sensitive narrow therapeutic index CYP3A4 substrate and which had been identified as a common co-medication in exacerbating patients, indicated a negligible risk using static mechanistic models. It is of significant note that without the PBPK model for nemiralisib, a CYP3A4 perpetrator clinical drug interaction study would be needed as part of the clinical development plan. The effort to develop, validate and apply such models is justified through reductions in unnecessary clinical trials, less subjects exposed to investigational drugs and future cost savings.

The impact of nemiralisib on drug transporters P-gp, BCRP, OAT1, OAT3, OATP1B1, OATP1B3, OCT2, MATE1 and MATE2-K was also studied in vitro. With the exception of OAT1 and OAT3, nemiralisib was a potent inhibitor of all these transporters, with IC_{50} values ranging 0.0260-3.03 µM. In 4 out of the 9 values, the potency with nemiralisib was higher than that observed for the positive control (Supplementary Table S9). The potential for nemiralisib to alter the clinical drug exposure of co-medications, whose disposition is dependent on these drug transporters, was assessed using basic equations as described by the EMA (2013) and FDA (2017b). Despite the high in vitro potencies, no systemic DDI risk was predicted up to maximum nemiralisib inhalation dose of 750 ug.

Interpretation of the nemiralisib in vitro inhibition data support the notion that the risk of perpetrator drug interactions is negligible for low dose inhaled molecules. This is nicely illustrated by the data for MATE1 and MATE2-K where IC_{50} values of 0.0260 and 0.0545 µM were >100 fold more potent than the cimetidine positive control making nemiralisib one of the most potent MATE inhibitor ever described. Despite

this, no threshold of concern was triggered when applying approaches recommended in regulatory guidelines. Although the risk of perpetrator drug interactions can be considered negligible for low dose inhalation molecules, CYP and transporter inhibition data should still be contextualized against clinical exposures using the framework outlined in guidance documents. It is prudent, therefore, to generate such inhibition data ahead of studies in patient populations, even for low dose inhalation molecules in order to defend the inclusion of common co-medications in clinical trial design and avoid any potential delay to the clinical trial approval process. Corresponding victim drug interaction risks cannot be discharged using the same “low dose inhalation” argument where a variety of factors come into play. These include the type of dose limiting toxicity, potency, therapeutic index, competing pathways, and enzyme kinetics. In the case of nemiralisib, a CYP3A4 victim clinical drug interaction study was needed to support the inclusion of macrolide antibiotics in special patient groups. Regulatory authorities expect to see a consideration of both victim and perpetrator risks aligned to regulatory guidance and the holistic approach used to assess the DDI risk with inhaled nemiralisib, in our view, addressed these regulatory requirements.

In conclusion, using an integrated in silico, in vitro and clinical approach, we have shown that any clinically significant DDI with nemiralisib are unlikely and that a range of common-comedications can be allowed safely into patient clinical study designs. Whilst inhaled drugs are expected to have low systemic exposure, it remains prudent to follow regulatory guidance including the tiered approach for perpetrator interactions. An integrated DDI assessment should be conducted for inhaled molecules and should include consideration of any co-medications relevant for the specific therapeutic area, in vitro perpetrator liabilities and victim investigations.

DMD Fast Forward. Published on February 2, 2020 as DOI: 10.1124/dmd.119.089003
This article has not been copyedited and formatted. The final version may differ from this version.

Acknowledgements

The authors would like to thank Azmina Mather who was the GSK study monitor for the drug transporter assays, and Jon Robertson, GSK, for reviewing the statistical analyses reported in the manuscript.

Editorial support was provided by Kate Hollingworth of Continuous Improvement Ltd and funded by GSK.

Availability of data and materials

Information on GSK's data sharing commitments and requesting access can be found at: https://www.clinicalstudydatarequest.com

Authorship Contributions

Participated in research design: AP, RW, AWH, KST, MT, HT, APC, MM

Conducted experiments: KST, HT, MT

Performed data analysis: AP, RW, KST, MT, HT, KR, MM

Wrote or contributed to the writing of the manuscript: All authors

References

Andersen M, Sarangapani R, Gentry R, Clewell H, Covington T, and Frederick CB. (2000) Application of a hybrid CFD-PBPK nasal dosimetry model in an inhalation risk assessment: an example with acrylic acid. *Toxicology Sciences* 57: 312-325.

Asgharian B, Price OT, and Hofmann W (2006) Prediction of particle deposition in the human lung using realistic models of lung ventilation. *J Aerosol Sci* 37: 1209-1221.

Asgharian B, Miller FJ, and Subramaniam RP (1999) Dosimetry software to predict particle deposition in humans and rats. *CIIT Activities* 19: 1-6.

Backman JT, Kivisto KT, Olkkola KT and Neuvonen PJ (1998) The area under the plasma concentration-time curve for oral midazolam is 400-fold larger during treatment with itraconazole than with rifampicin. *Eur J Clin Pharmacol.* 54: 53–58.

Begg M, Wilson R, Hamblin JN, Montembault M, Green J, Deans A, Amour A, Worsley S, Fantom K, Cui Y, Dear G, Ahmad S, Kielkowska A, Clark J, Boyce M, Cahn A, and Hessel EM (2019) Relationship between pharmacokinetics and pharmacodynamic responses in healthy smokers informs a once daily dosing regimen for nemiralisib. *J Pharmacol Exp Ther* 369: 443-453.

Bloomer J, Dermanov G, Dumont E, Ellens H, and Matheny C (2013) Optimising the in vitro and clinical assessment of drug interaction risk by understanding co-medications in patient populations. *Expert Opin Drug Metab Toxicol* 9: 737-751.

Boger E and Friden M (2019) Physiolologically based pharmacokinetic/ pharmacodynamic modeling accurately predicts the better bronchodilatory

effect of inhaled versus oral salbutamol dosage forms. *J Aerosol Med Pulm Drug Deliv* 32: 1-12.

Boger E and Wigstrom O (2018) A partial differential equation approach to inhalation physiologically based pharmacokinetic modelling. *CPT Pharmacometrics Syst Pharmacol* 7: 638-646.

Borghardt JM, Weber B, Staab A, and Kloft C (2015) Pharmacometric models for characterizing the pharmacokinetics of orally inhaled drugs. *AAPS J* 17: 853-870.

Cahn A, Hamblin JN, Begg M, Wilson R, Dunsire L, Sriskantharajah S, Montembault M, Leemereise CN, Galinanes-Garcia L, Watz H, Kirsten AM, Fuhr R, and Hessel EM (2017) Safety, pharmacokinetics and dose-response characteristics of GSK2269557, an inhaled PI3Kδ inhibitor under development for the treatment of COPD. *Pulm Pharmacol Ther* 46: 69-77.

Down K., Amour A, Baldwin IR, Cooper AJW, Deakin AM, Felton LM, Guntrip SB, Hardy C, Harrison ZA, Jones KL, Jones P, Keeling SE, Le J, Livia S, Lucas F, Lunniss CJ, Parr NJ, Robinson E, Rowland P, Smith S, Thomas DA, Vitulli G, Washio Y, and Hamblin JN (2015) Optimization of Novel Indazoles as Highly Potent and Selective Inhibitors of Phosphoinositide 3-Kinase δ for the Treatment of Respiratory Disease. *J Med Chem* 58: 7381-7399.

European Medicines Agency (EMA), Guideline on the investigation of drug interactions, Committee for Human Medicinal Products (CHMP), 2012, CPMP/EWP/560/95/Rev. 1 Corr. 2.

Foisy MM, Yakiwchuk EMK, Chiu I, and Singh AE (2008) Adrenal suppression and Cushings syndrome secondary to an interaction between ritonavir and fluticasone: a review of the literature. *HIV Medicine*. 9: 389-396.

Gorski JC, Jones DR, Haehner-Daniels BD, Hamman MA, O'Mara EM Jr, and Hall SD (1998) The contribution of intestinal and hepatic CYP3A to the interaction between midazolam and clarithromycin. *Clin Pharmacol Ther* 64: 133-43.

Harrell AW, Wilson R, Yau Lun Man, Riddell K, Jarvis E, Young G, Chambers R, Crossman L, Georgiou A, Pereira A, Kenworthy D, Beaumont C, Marotti M, Wilkes D, Hessel EM, and Fahy WA (2019) An innovative approach to characterize clinical ADME and pharmacokinetics of the inhaled drug nemiralisib using an intravenous microtracer combined with an inhaled dose, and an oral radiolabel dose in healthy male subjects. *Drug Metab Dispos* 47: 1457-1468.

Ke AB, Zamek-Gliszczynski MJ, Higgins JW, and Hall SD (2014) Itraconazole and clarithromycin as ketoconazole alternatives for clinical CYP3A inhibition studies. *Clin Pharmacol Ther* 95: 473-476.

Kempsford R, Allen A, Bal J, and Tombs L (2013) The effect of ketoconazole on the pharmacokinetics and pharmacodynamics of inhaled fluticasone furoate and vilanterol trifenatate in healthy subjects. *Br J Clin Pharmacol* 75: 1478-1487.

Lawrence SK, Nguyen D, Bowen C1, Richards-Peterson L, and Skordos KW (2014) The metabolic drug-drug interaction profile of Dabrafenib: in vitro investigations and quantitative extrapolation of the P450-mediated DDI risk. *Drug Metab Dispos* 42: 1180-1190.

Olkkola KT, Backman JT, and Neuvonen PJ (1994) Midazolam should be avoided in patients receiving the systemic anti-myotics ketoconazole and itraconazole. *Clin Pharmacol Ther* 55: 481-485.

Shebley M, Sandhu P, Emami Riedmaier A, Jamei M, Narayanan R, Patel A, Peters SA, Reddy VP, Zheng M, de Zwart L, Beneton M, Bouzom F, Chen J, Chen Y, Cleary Y, Collins C, Dickinson GL, Djebli N, Einolf HJ, Gardner I, Huth F, Kazmi F, Khalil F, Lin J, Odinecs A, Patel C, Rong H, Schuck E, Sharma P, Wu SP, Xu Y, Yamazaki S, Yoshida K, and Rowland M (2018) Physiologically Based Pharmacokinetic Model Qualification and Reporting Procedures for Regulatory Submissions: A Consortium Perspective. *Clin Pharmacol Ther* 104: 88-110.

Sirmans SM (1988) Effect of calcium channel blockers on theophylline disposition. *Clin Pharmacol Ther* 44: 29-34.

Stringer KA, Mallet J, Clarke M, and Lindenfeld JA (1992) The effect of three different oral doses of verapamil on the disposition of theophylline. *Eur J Clin Pharmacol* 43: 35-8.

Somers GI, Lindsay N, Lowdon BM, Jones AE, Freathy C, Ho S, Woodrooffe AJM, Bayliss MK, and Manchee GR (2007) A comparison of the expression and metabolizing activities of phase I and II enzymes in freshly isolated human lung parenchymal cells and cryopreserved human hepatocytes. *Drug Metab Dispos* 35: 1797-1805.

Tjia JF, Colbert J, and Back DJ (1996) Theophylline metabolism in human liver microsomes: inhibition studies. *J Pharmacol Exp Ther* 276: 912-917.

Wilson R, Jarvis E, Montembault M, Hamblin JN, Hessel EM, and Cahn A (2018) Safety, Tolerability, and Pharmacokinetics of Single and Repeat Doses of Nemiralisib Administered via the Ellipta Dry Powder Inhaler to Healthy Subjects. *Clin Ther* 40: 1410-1417.

Wilson R, Templeton A, Leemereise C, Eames R, Banham-Hall E, Hessel EM, and Cahn A (2019) Safety, tolerability and pharmacokinetics of a new formulation of nemiralisib administered via the Ellipta dry powder inhaler to healthy individuals. *Clin Ther* 41(6): 1214-1220.

U.S. Department of Health and Human Services Food and Drug Administration (FDA), Drug interaction studies – study design, data analysis and implications for dosing and labelling, draft guidance, Center for Drug Evaluation and Research (CDER), 2006.

U.S. Department of Health and Human Services Food and Drug Administration (FDA), Clinical drug interaction studies - study design, data analysis, and clinical implications, guidance for industry, draft guidance, Center for Drug Evaluation and Research (CDER), 2017a.

U.S. Department of Health and Human Services Food and Drug Administration (FDA), In vitro metabolism and transport-mediated drug-drug interaction studies, guidance for industry, draft guidance, Center for Drug Evaluation and Research (CDER), 2017b.

Footnotes

This study was funded by GlaxoSmithKline.

AWH, RW, KR, AG, APC are GSK employees and hold GSK shares

AP, KST, MT, HT, MM are GSK employees

EMH is a GSK employee and holds GSK shares and is on patents pertaining to the research discussed in the manuscript

DMD Fast Forward. Published on February 2, 2020 as DOI: 10.1124/dmd.119.089003
This article has not been copyedited and formatted. The final version may differ from this version.

Figure legends

Figure 1: Study schematic

Figure 2: Median nemiralisib concentration time plot from a clinical drug interaction study investigating the effect of oral itraconazole (a potent CYP3A4 and Pgp inhibitor) on the pharmacokinetics of inhaled nemiralisib.

Nemiralisib concentration data are compared between a single inhalation administration of 100 µg of nemiralisib when dosed alone (without itraconazole) and following repeated oral administration of 200 mg itraconazole (with itraconazole). X axis is plotted to nominal sample times and not actual sampled times.

Figure 3: SimCYP® simulated (lines) and observed (symbols) plasma profiles after A) 10 µg intravenous dose, B) 800 µg oral dose, C) 1000 µg inhaled dose of nemiralisib in healthy volunteers

DMD Fast Forward. Published on February 2, 2020 as DOI: 10.1124/dmd.119.089003
This article has not been copyedited and formatted. The final version may differ from this version.

Table 1: Total percent contribution of individual P450 enzymes to nemiralisib metabolism

rCYP Enzyme	% contribution to overall metabolism
CYP1A2	0.9
CYP2C8	2.1
CYP2C9	1.8
CYP2C19	< 0.1
CYP2D6	0.3
CYP3A4	94.9

Abbreviations: rCYP: recombinant CYP

DMD Fast Forward. Published on February 2, 2020 as DOI: 10.1124/dmd.119.089003
This article has not been copyedited and formatted. The final version may differ from this version.

Table 2: Quantitative DDI Victim Risk Assessment for Nemiralisib: CYP Inhibition

Cytochrome P450 (CYP)	Fold Change in IC_{50}[a]	Inactivation parameters		Is a DDI risk predicted?
		K_I (µM)	k_{inact} (min^{-1})	
1A2	2.7	No inactivation of CYP1A2		
2B6	1.9	2.0	0.014	No[b]
2C8, 2C9, 2C19 & 2D6	<1.5			
3A4	>7.9[d]	4.2	0.034	No[c]

a. A less than 1.5-fold change in IC_{50} is deemed a low risk of DDI and no additional inactivation data were generated
b. Risk discharged using static mechanistic models described by FDA (2017b) and EMA (2012).
c. Risk discharged using physiologically based pharmacokinetic modelling.
d. Worst case

Abbreviations: DDI: drug-drug interaction; IC_{50}: half maximal inhibitory concentration; K_i: inactivator concentration to achieve half-maximal inactivation rate; k_{inact}: maximal rate constant of inactivation

Table 3: Summary of statistical analysis derived nemiralisib pharmacokinetic parameters following inhalation administration of nemiralisib alone and inhaled nemiralisib with oral itraconazole

PK parameter	Treatment	N	n	Adjusted geometric mean (90% CI)	Ratio of adjusted geometric means (90% CI), nemiralisib vs. nemiralisib with itraconazole	Mean squared error
$AUC_{0\text{-}inf}$ (h*pg/mL)	Nemiralisib 100 µg single dose	20	20	3199.0 (2874.7, 3559.9)	2.01 (1.81, 2.22)	0.0253
	Nemiralisib 100 µg single dose with itraconazole 200 mg repeat dose	20	14	6413.4 (5695.9, 7221.3)		
C_{max} (pq/mL)	Nemiralisib 100 µg single dose	20	20	478.7 (416.4, 550.3)	0.802 (0.690, 0.933)	0.0762
	Nemiralisib 100 µg single dose with itraconazole 200 mg repeat dose	20	20	384.0 (334.0, 441.4)		

Abbreviations: $AUC_{0\text{-}inf}$: area under the plasma concentration-time curve time zero (pre-dose) extrapolated to infinite time; C_{max}: maximum observed plasma concentration, CI: confidence interval; N: number of subjects; n: number of evaluable subjects

Table 4: Simulated and observed nemiralisib exposure ratio following inhalation administration in the presence of potent CYP3A4 inhibitor Itraconazole administered by the oral route.

	Simulated Geometric mean ratio (5^{th} and 95^{th} centile)	**Observed Geometric mean ratio (90% CI of Ratio) *(min - max)***
N	400 (20 trials each with 20 subjects)	20
C_{max} ratio	1.0 (0.99-1.01)	0.802 (0.690-0.933)
$AUC_{0\text{-}inf}$ ratio	2.25 (1.66-3.36)	2.01 (1.81-2.24) *(1.48 - 3.24)**

Abbreviations: $AUC_{0\text{-}inf}$: area under the plasma concentration-time curve time zero (pre-dose) extrapolated to infinite time; C_{max}: maximum observed plasma concentration, CI: confidence interval
*N=14

Table 5: Prospective drug interaction predictions with CYP3A4 inhibitors Clarithromycin and Erythromycin

	Simulated ratio with Clarithromycin	Simulated ratio with Erythromycin
Simulated individuals	1000	1000
Reference for study design	Gorski 1998	Olkkola 1993
Simulated study design	500 mg BID for 7 days and 4 mg midazolam on day 7 (2 hrs after the first dose of Clarithromycin)	500 mg TID Erythromycin for one week and 15 mg midazolam on day 6 (2 hrs after 2nd dose of the day)
Age range for simulated individuals[1]	21-62	21-62
Simulated gender ratio[1]	Males	Males
$AUC_{0\text{-}inf}$ Geometric mean ratio (5^{th} and 95^{th} centile)	1.71 (1.27-2.48)	1.67 (1.22-2.40)

Abbreviations: $AUC_{0\text{-}inf}$: area under the plasma concentration-time curve time zero (pre-dose) extrapolated to infinite time; BID: twice a day; TID: three times a day

[1]Demographics based on NCT033984

Fig. 1

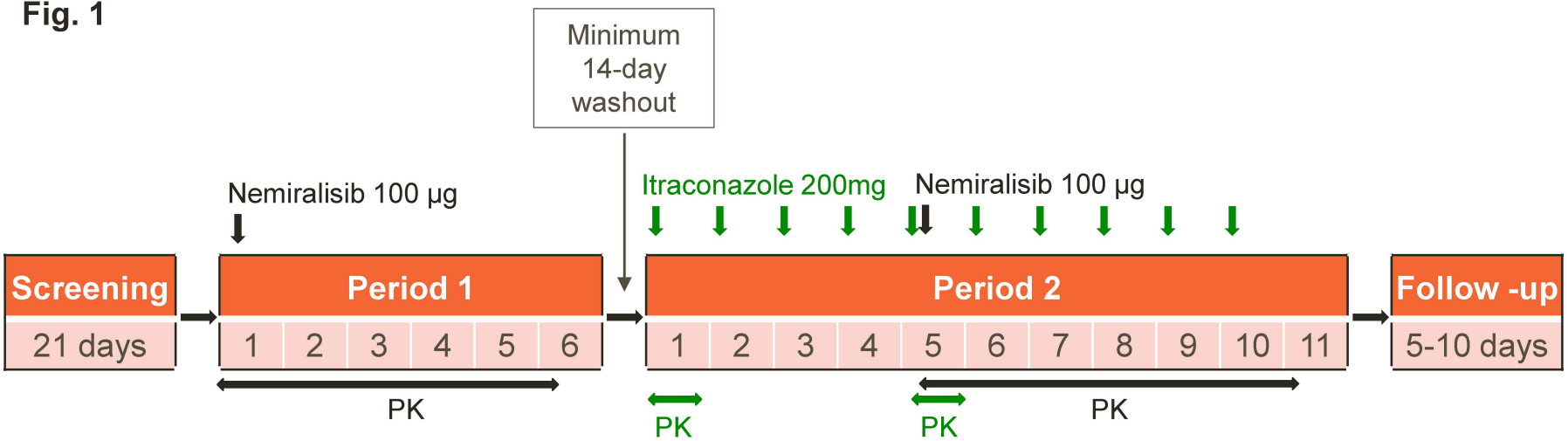
Minimum
14-day
washout
Nemiralisib 100 µg
Itraconazole 200mg
Nemiralisib 100 µg
Screening
21 days
Period 1
1 2 3 4 5 6
Period 2
1 2 3 4 5 6 7 8 9 10 11
Follow -up
5-10 days
PK
PK
PK
PK

Fig. 2

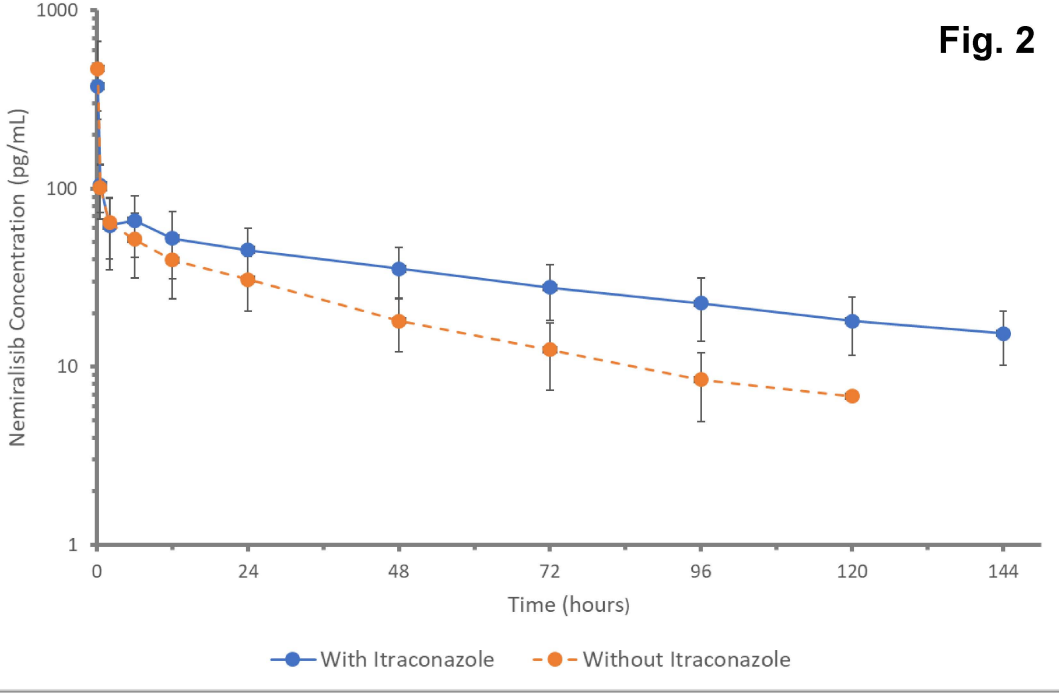
1000
100
10
1
Nemiralisib Concentration (pg/mL)
0
24
48
72
96
120
144
Time (hours)
With Itraconazole
Without Itraconazole

Fig. 3A

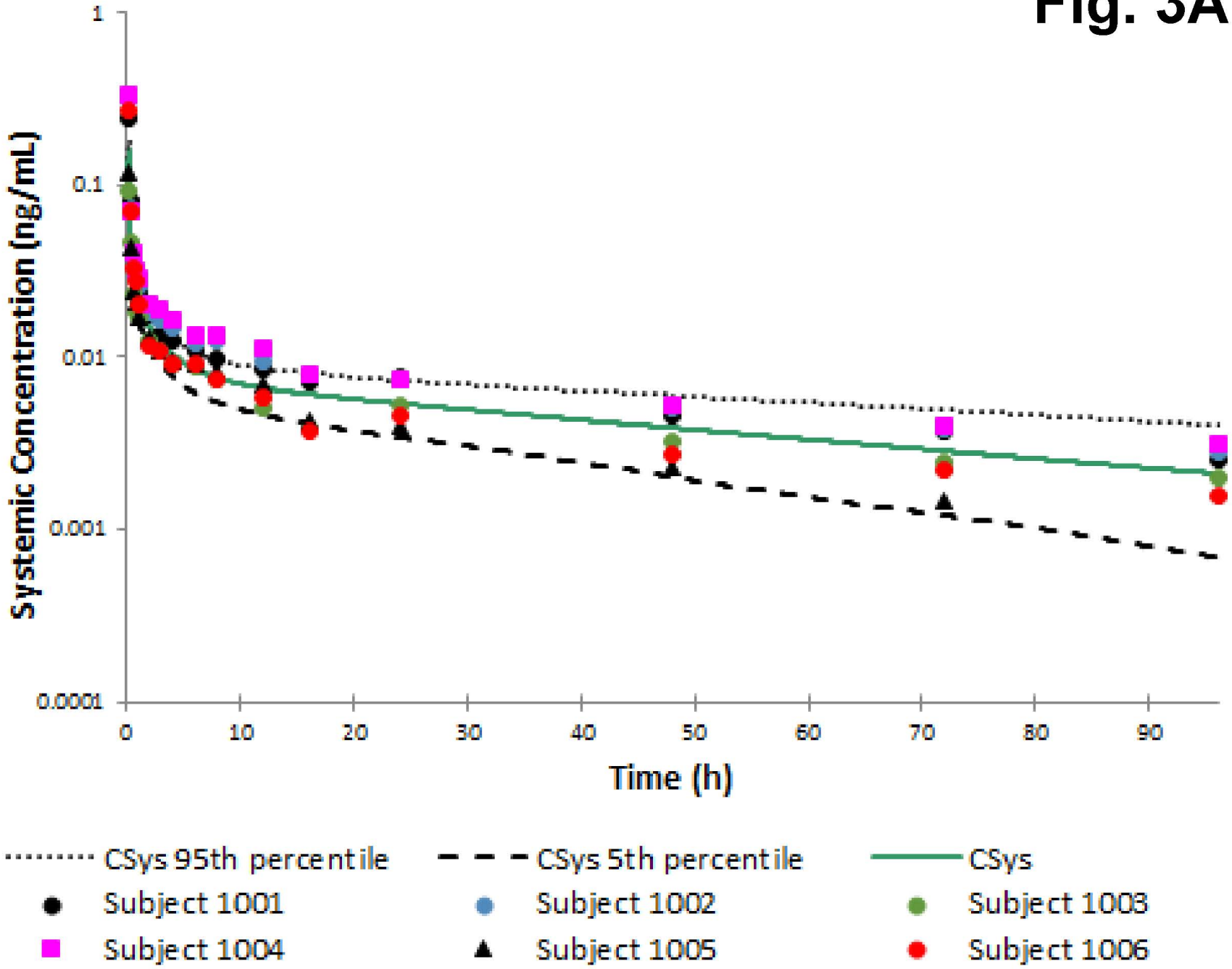
Systemic Concentration (ng/mL)
1
0.1
0.01
0.001
0.0001
0
10
20
30
40
50
60
70
80
90
Time (h)
CSys 95th percentile
CSys 5th percentile
CSys
Subject 1001
Subject 1002
Subject 1003
Subject 1004
Subject 1005
Subject 1006

Fig. 3B

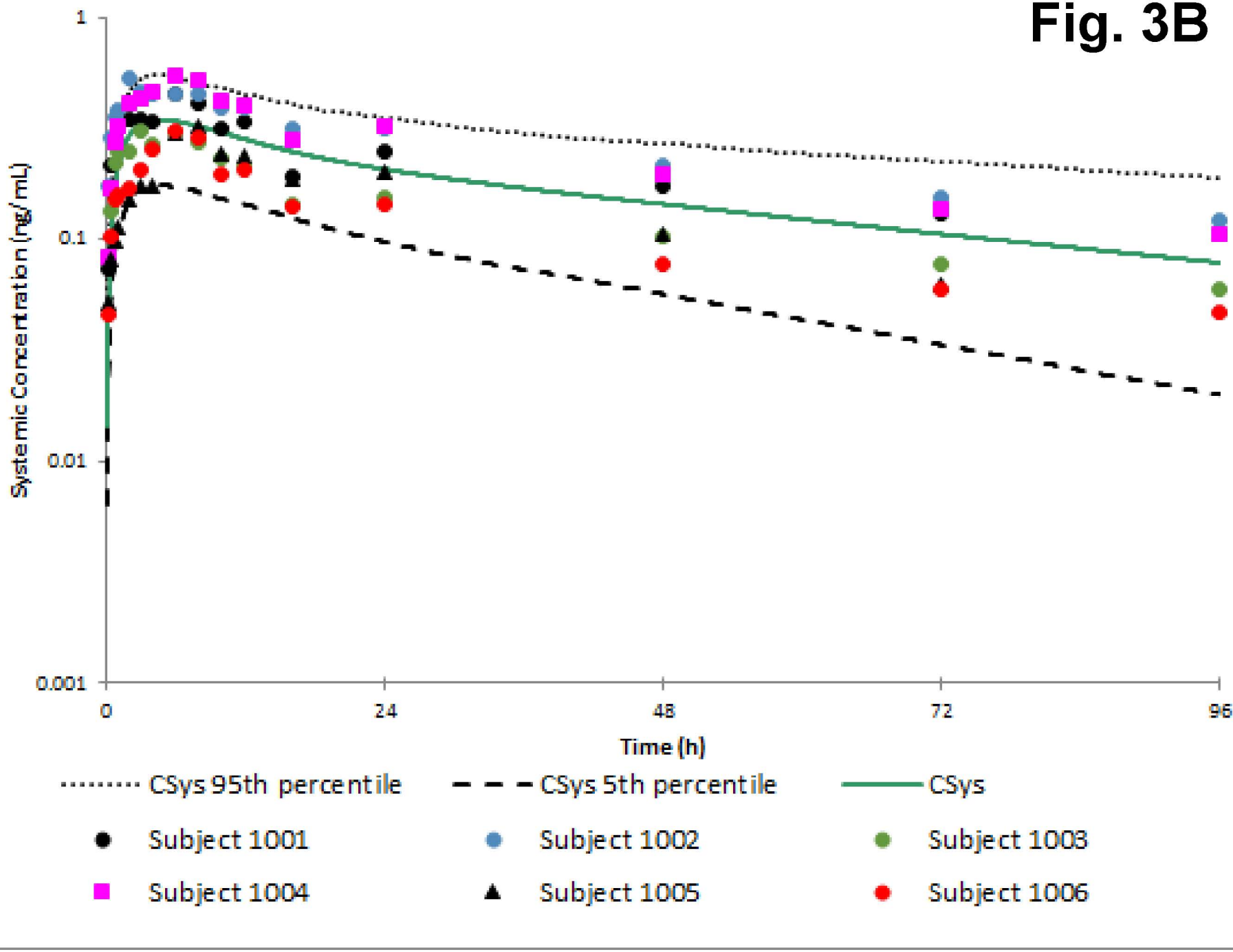
1
0.1
0.01
0.001
Systemic Concentration (ng/mL)
0
24
48
72
96
Time (h)
CSys 95th percentile
CSys 5th percentile
CSys
Subject 1001
Subject 1002
Subject 1003
Subject 1004
Subject 1005
Subject 1006

Figure 3C